Toward a Square Grid Polymer: Electrochemistry of Tentacled Tetragonal Star Connectors, $C_4R_4-Co-C_5(HgY)_5$, on Mercury

Thierry Brotin,[†] Lubomír Pospíšil,[‡] Jan Fiedler,[‡] Benjamin T. King,[†] and Josef Michl*,[†]

Department of Chemistry and Biochemistry, University of Colorado, Boulder, Colorado 80309-0215, and J. Heyrovský Institute of Physical Chemistry, Dolejškova 3, 18223 Prague 8, Czech Republic

Received: July 31, 1998

Electrochemical reduction of cyclobutadienecyclopentadienylcobalt derivatives, $C_4R_4-Co-C_5(HgY)_5$ [R = C_6H_5-, Y = −SMe (**3**), −SCOMe (**4**), $-SCH_2CH_2SCH_3$ (**5**), $-SCH_2CH_2SCOCH_3$ (**6**); R = *p*-$EtOCOC_6H_4-$, Y = −SEt (**7**), −SCOMe (**8**), $-SCH_2CH_2SCH_3$ (**9**), $-SCH_2CH_2SCOCH_3$ (**10**)], and the parent $C_4R_4-Co-C_5H_5$ [R = C_6H_5- (**11**) and R = *p*-$EtOCOC_6H_4-$ (**12**)] has been examined. Reversible one-electron "metal-centered" reduction of **11** (−2.24 V vs Ag/AgCl) yields a stable radical anion. In **12**, it takes place at −1.70 V. In **3**−**10**, similar metal-centered reduction occurs irreversibly, accompanied by an adsorption pre-wave at −0.7 to −1.15 V. We propose that the radical anion loses a −HgSX substituent soon after it is formed. Electrochemical cleavage of the substituents occurs before the metal-centered reduction in **4** and **8** and afterward in the others. The cleaved thiolate fragments yield an anodic peak. In all compounds with ester groups, ester reduction is observed at −2.1 to −2.5 V.

Introduction

The overall scheme proposed[1] for the synthesis of square grid polymers by interfacial synthesis calls for monomeric modules consisting of a cross-shaped connector mounted on a pedestal that carries three or more tentacles with functionalities that have high affinity for the surface of a liquid such as mercury. The structures that we have initially chosen for this purpose are organometallic sandwich complexes and, among others, tetra-*p*-substituted tetraphenylcyclobutadienecyclopentadienylcobalt complexes. The five mercurio substituents are introduced onto the cyclopentadienyl (Cp) ring of these complexes with mercuric trifluoracetate to afford **1** and **2** in good yield, and the trifluoroacetate moiety is subsequently easily displaced by thiol-terminated chains to attach almost any kind of desired structure.[2]

We have exploited this facile access for the preparation of a series of pentatentacled derivatives of **1** and **2** and hope to find the potential ranges within which they adhere firmly to a mercury surface. The simpler model compounds **3**−**6** with unsubstituted phenyl groups on the cyclobutadiene (Cb) ring are useless for future grid formation, but should help us unravel the electrochemical behavior of the more complex compounds **7**−**10**. Of the two choices of adhesive groups, the alkylthio group, present in **3**, **5**, **7**, and **9**, was previously found to adsorb firmly on gold,[3] and on mercury at positive potentials.[4] The potential range in which the acetylthio groups of **4**, **6**, **8**, and **10** will adsorb on mercury is unknown. In principle, the acetylthio group also offers an opportunity for hydrolytic conversion into a thiol group, which will surely adhere firmly to both metals, but the free thiols appear to be unstable with respect to thiol ligand exchange on mercury. They will probably have to be generated from adsorbed acetylthio derivatives in situ, and we have not examined them so far.

Because of the multitude of electroactive groups in the molecules, an examination of oxidation−reduction properties and comparison with the parent structures **11** and **12** seemed advisable before an investigation of adsorption properties. The results are reported presently, and the adsorption behavior will be described separately.[5]

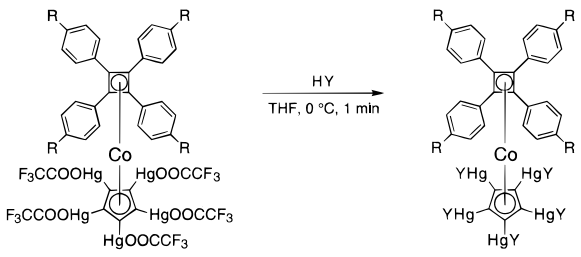

	R:	Y:
1, R = H		
2, R = COOEt		
	3 - H	- SMe
	4 - H	- SCOMe
	5 - H	- SCH_2CH_2SMe
	6 - H	- SCH_2CH_2SCOMe
	7 - COOEt	- SEt
	8 - COOEt	- SCOMe
	9 - COOEt	- SCH_2CH_2SMe
	10 - COOEt	- SCH_2CH_2SCOMe

Little is known about the electrochemical behavior of cyclobutadienecyclopentadienylcobalt complexes. The unsubstituted parent compound, CbCoCp, undergoes two irreversible oxidation processes at +0.79 and +1.14 V vs saturated calomel electrode (SCE),[6] but its reduction has apparently not been examined. A derivative with four alkyl substituents on the Cb ring shows a reversible oxidation wave at +0.46 V vs SCE,[7] and some more complicated structures with two Co centers have also been investigated,[8] but once again, the reduction seems not to have been examined. A related cation, tetraphenylcyclobutadiene(benzene)cobalt(I),[9] is reduced reversibly at −1.22 V vs SCE, then irreversibly at −1.75 V and finally again reversibly at −2.06 V, and the product is oxidized irreversibly at −0.23 V. A replacement of the four phenyl substituents with

[†] University of Colorado.
[‡] J. Heyrovský Institute of Physical Chemistry.

10.1021/jp983242i CCC: $15.00
Published on Web 11/05/1998

four methyl groups changes the reduction pattern; only one irreversible reduction at −1.92 V and one irreversible oxidation at −0.80 V are observed. The formation of a protonated cyclobutenyl complex was postulated as a reason for the irreversibility and for the appearance of an oxidation wave.[9]

Experimental Section

Methods. Electrochemical measurements were done using a home-built electrochemical system for cyclic voltammetry, phase-sensitive AC polarography, and DC polarography. It consisted of a fast rise-time potentiostat and a lock-in amplifier (EG&G, model 5209). The instruments were interfaced to a 486-type personal computer via an IEEE interface card (PC-Lab, AdvanTech, model PCL-848) and a data acquisition card (PCL-818) using 12-bit precision. The source of the AC signal for the cell was derived from the internal oscillator of the lock-in amplifier. The amplitude was attenuated to 5 mV (p−p). The impedance spectra were measured in the range 1 Hz to 100 kHz using a frequency spectrum analyzer (Stanford Research, model SRS760) connected to a potentiostat (EG&G Princeton Applied Research, model 263). A three-electrode electrochemical cell was used. Ag/AgCl/1M LiCl served as a reference electrode and was separated from the test solution by a salt bridge. The half-wave potential of the ferrocene couple vs our reference electrode was +0.562 V. The working electrode was a valve-operated static mercury electrode (SMDE2, Laboratorní Přístroje, Prague) with an area of 1.32×10^{-2} cm^{-2}. The auxiliary electrode was a cylindrical platinum net. Oxygen was removed from the solution by passing a stream of argon. THF was distilled under the inert atmosphere prior to use. Preparative electrolysis of **5** was performed on a Hg pool electrode of a 3.8 cm^2 area. The anode and cathode spaces were separated by a horizontal salt bridge of 8 cm terminated on both sides with a glass frit. The solution was stirred with a magnetic stirrer. Potential was controlled with a EG&G model 273 potentiostat that also measured the charged that passed. Polarographic or voltammetric curves were recorded prior to and after the electrolysis. After completed electrolysis, the solvent was removed under reduced pressure and the resulting solid was triturated with benzene. The extract was evaporated to dryness and again triturated with benzene, and the process was repeated one more time. Final purification of the reduction product was by chromatography on silica gel with hexanes/benzene. Product identification was done by comparison of ^1H NMR and of TLC R_f values with those of authentic standards.

Melting points were recorded using a Melt temp II apparatus (Laboratory Devices). Unless specified otherwise, ^1H and ^{13}C NMR spectra were obtained in DMSO-d_6 solution with a Varian VXR-300 S spectrometer at 299.949 and 75.428 MHz respectively, using Me_4Si as an external reference. IR spectra were obtained with a Nicolet 800 FT-IR spectrometer. Electron impact (EI) and fast atom bombardment (FAB) mass spectra were obtained with a VG 7070 EQ-HF hybrid tandem mass spectrometer. Microanalyses were performed by Desert Analytics, Tucson, AZ, and the Microanalytical Laboratory at the University of California, Berkeley.

Materials. All reagents were purchased from Aldrich, except for ethyl 4-iodobenzoate (TCI America), and were used as supplied. 2-Methanethioethanethiol was prepared by a reported[10] procedure. 4,4′-Di(ethoxycarbonyl)phenylacetylene[2] was purified by column chromatography on silica gel. Tetrasubstituted tetraphenylcyclobutadienecyclopentadienylcobalt complexes were prepared by the method of Rausch[11] as reported previously,[2] using freshly distilled $CpCo(CO)_2$. All solvents were analytical grade and were freshly distilled before use.

2-Acetylthioethanethiol. To a stirred solution of $KHCO_3$ (10.63 g, 0.106 mol) in water (100 mL), a solution of 1,2-ethanedithiol (10 g, 0.106 mol) in diethyl ether (60 mL) was added. The mixture was cooled to 0 °C, and acetic anhydride (10 mL) was slowly added in one portion. The mixture was stirred at room temperature for 45 min, cooled at 0 °C, and quenched with 5 N HCl (30 mL). The organic material was extracted with diethyl ether, and the extract was washed with water and dried over Na_2SO_4. Evaporation of diethyl ether gave rise to 2 g (11%, mp 68−69 °C, lit.[12] 68.5 °C) of 1,2-bisacetylthioethane, which was collected on a frit. The residual oil was chromatographed on silica gel (ether/pentane, 10/90). The desired compound was eluted first. After the solvent was evaporated, the oily product was distilled twice to give the pure product as a colorless oil (1.2 g, 8%): bp 87−90 °C/17 Torr (lit.[13] 92 °C/17 Torr); ^1H NMR ($CDCl_3$) δ 1.59 (t, 1H, J = 8.4 Hz), 2.32 (s, 3 H, $COCH_3$), 2.655 (m, 2 H, CH_2), 3.07 (m, 2 H, CH_2); ^{13}C {^1H} NMR ($CDCl_3$) δ 24.60 (CH_2), 30.60 (CH_2), 33.10 (CH_3), 195.13 (CO); IR (neat, cm^{-1}) 2927 (ν −CH, w), 2564 (ν SH, w), 1691 (ν C═O, s), 1424 (δ CH_3, CH_2, s), 1354 (δ CH_3, s), 1273 (m), 1215 (m), 1134−1105 (s), 954 (s), 702 (w), 624 (ν S−CO, m); MS (EI+) *m*/*z* (rel int.) 136 (M, 7%), 77 (14%), 59 (32%), 43 (100%, CH_3-CO+), 27 (28%, CH_2═CH+), 15 (29%, CH_3+). Anal. Calcd for $C_4H_8S_2O$: C, 35.27; H, 5.92. Found: C, 35.42; H, 6.03.

Tetraphenylcyclobutadienepentakis(methylthiomercurio)-cyclopentadienylcobalt (3). A solution of sodium thiomethoxide (0.035 g, 0.45 mmol) was dissolved in a minimum of water and added under argon in one portion to a solution of **1** (0.152 g, 0.074 mmol) in THF (6 mL) cooled to 0 °C. After being stirred for 1 min at 0 °C, a mixture of EtOH (5 mL) and hexanes (50 mL) was added, and stirring was continued for 5 min at room temperature. The precipitate was collected on a frit, washed with copious EtOH and then hexanes, and dried in air (85 mg, 66%): mp >250 °C (dec); ^1H NMR δ 7.64 (m, 8 H, phenyl), 7.20 (m, 12 H, phenyl), 2.12 (s, 15 H, CH_3); ^{13}C {^1H} NMR δ 10.01 (CH_3), 73.34 (Cb), 125.30 (Cp), 126.33, 128.21, 128.29, 137.34 (Ph); IR (KBr, cm^{-1}) 3054 (ν ═CH, vw), 2916 (ν −CH, w), 1630 (ν Ph, vw), 1596 (ν Ph, w), 1497 (m), 1441 (w), 1311 (w), 1118 (w), 695 (m), 559 (m). Useful FAB MS could not be obtained due to low solubility. Anal. Calcd for $C_{38}H_{35}S_5Hg_5Co$: C, 26.63; H, 2.06. Found: C, 26.88; H, 2.08.

General Procedure for Reactions of 1 and 2 with Thiols. A solution of thiol dissolved in a minimum of THF was added in one portion to a solution of **1** or **2** in THF cooled to 0 °C under argon. The mixture was stirred for 1 min, and a mixture of hexanes was added to quench the reaction and to precipitate the desired product. Stirring was continued for 5 min at room temperature. The compounds were collected on a frit, washed with copious hexanes, and purified by precipitation (**3, 5, 6**) or recrystallization (**4, 7, 8**−**10**). Chromatography on silica gel or basic alumina under ordinary conditions caused partial decomposition. NMR spectra gave no indication of hindrance to rotation of the two decks relative to each other.

Tetraphenylcyclobutadienepentakis(acetylthiomercurio)-cyclopentadienylcobalt (4). Thiolacetic acid (0.19 g, 2.5 mmol) in THF (2 mL) was added to **1** (0.5 g, 0.25 mmol) in THF (8 mL). After precipitation with hexanes (50 mL), the product was purified by recrystallization from THF/EtOH (dark-red crystals, 0.25 g, 55%): mp 165−170 °C (dec); ^1H NMR δ 7.715 (m, 8 H, Ph), 7.19 (m, 12 H, Ph), 2.27 (s, 15 H, CH_3); ^{13}C {^1H} NMR δ 25.095 (CH_3), 74.28 (Cb), 123.19 (Cp), 126.42, 128.39, 128.58 (Ph), 137.10, 201.34 (CO); IR (KBr, cm^{-1}) 3056 (ν ═CH, vw), 2926 (ν −CH, vw), 1624 (br, ν C═O), 1497

(m), 1350 (m), 1114 (s), 952 (m), 708 (m), 635 (ν S−CO, s); MS (FAB+, 3-NOBA) *m*/*z* maximum calcd at 1854, found 1856. Anal. Calcd for $C_{43}H_{35}S_5Hg_5Co$·THF: C, 29.30; H, 2.25. Found: C, 29.15; H, 2.18.

Tetraphenylcyclobutadienepentakis(2-methylthioethanethiolmercurio)cyclopentadienylcobalt (5). **5** was synthesized from **1** (0.2 g, 0.098 mmol) in THF (5 mL) and 2-methylthioethanethiol (0.064 g. 0.58 mmol) in THF (1 mL). Hexanes (50 mL) were added to precipitate **5**, which was then redissolved in a minimum of THF, the solution was filtered through a filter paper, and addition of hexanes (40 mL) precipitated **5** as a yellow solid (0.119 g, 60%): mp 73−74 °C (dec); ^{1}H NMR δ 7.66 (m, 8 H, Ph), 7.20 (m, 12 H, Ph), 3.04 (broad t, 10 H, J = 6.6 Hz, CH_2), 2.63 (broad t, 10 H, J = 6.6 Hz, CH_2), 1.96 (s, 15 H, CH_3); ^{13}C {^{1}H} NMR δ 14.46 (CH_3), 26.76 (CH_3), 39.14 (CH_2), 73.42 (Cb), 126.20 (Cp), 126.38, 128.28, 128.35, 137.19 (Ph); IR (KBr, cm^{-1}) 3054 (ν =CH, vw), 2910 (ν −CH, w), 1629−1596 (ν Ph, w), 1497 (m), 1428 (w), 1260 (w), 1197 (w), 1118 (w), 705 (m), 558 (m); MS (FAB+, NOBA) *m*/*z* maximum calcd at 2014, found 2015. Anal. Calcd for $C_{48}H_{55}S_{10}Hg_5Co$: C, 28.62; H, 2.75. Found: C, 28.88; H, 2.80.

Tetraphenylcyclobutadienepentakis(2-acetylthioethanethiomercurio)cyclopentadienyl-cobalt (6). **6** was synthesized from **1** (0.2 g, 0.098 mmol) in THF (5 mL) and 2-acetylthioethanethiol (0.09 g, 0.66 mmol) in THF (1 mL). Addition of hexanes (50 mL) precipitated **6** (0.19 g, 90%): mp 65−70 °C (dec); ^{1}H NMR δ 7.63 (m, 8 H, Ph), 7.195 (m, 12 H, Ph), 2.85 (m, 20 H, C_2H_4), 2.31 (s, 15 H, CH_3); ^{13}C {^{1}H} NMR δ 27.10 (CH_2), 30.75 (CH_2), 34.42 (CH_3), 73.42 (Cb), 125.39 (Cp), 126.43, 128.25, 128.36, 137.31 (Ph), 195.00 (CO); IR (KBr, cm^{-1}) 3050 (ν =CH, vw), 2917 (ν −CH, vw), 1690 (ν C=O, s), 1596 (ν Ph, w), 1497 (m), 1352 (w), 1262 (w), 1202 (w), 1132 (s), 961 (w), 700 (m), 625 (ν S−CO, m), 559 (w); MS (FAB+, 3-NOBA) *m*/*z* maximum calcd at 2154, found 2154. Anal. Calcd for $C_{53}H_{55}S_{10}O_5Hg_5Co$: C, 29.55; H, 2.57. Found: C, 29.40; H, 2.47.

Thiol Exchange. An attempt to remove the acetyl groups from **6** with 0.2 N KOH in aqueous THF at room temperature gave complicated mixtures, presumably because the liberated thiol groups exchanged with those already attached to mercury. Evidence for such exchange was obtained from reaction of **6** with 20 equiv of ethanethiol. After 5−10 min at room temperature, the product was separated, and its NMR clearly showed that some of the initially present tentacles had been replaced by ethanethiol.

Tetra(4-ethoxycarbonylphenyl)cyclobutadienepentakis(ethylthiomercurio)cyclopentadienylcobalt (7). **7** was synthesized from **2** (0.2 g, 0.086 mmol) in THF (5 mL) and ethanethiol (0.032 g, 0.515 mmol). Hexanes (50 mL) precipitated **7**, which was redissolved in a minimum of THF, filtered through a filter paper, precipitated with hexanes (50 mL) as a yellow-orange powder (0.112 g, 63%) and recrystallized from DMSO (dark-red crystals): mp 185−190 °C (dec); ^{1}H NMR δ 7.82 (d, 8 H, J = 9.0 Hz, Ph), 7.75 (d, 8 H, J = 9.0 Hz, Ph), 4.30 (q, 8 H, J = 6.9 Hz, OCH_2), 2.69 (q, 10 H, J = 7.2 Hz, SCH_2), 1.30 (t, 12 H, J = 6.9 Hz, CH_3), 1.12 (t, 15 H, J = 7.2 Hz, CH_3); ^{13}C {^{1}H} NMR δ 14.21 (CH_3), 21.42 (CH_3), 22.31 (SCH_2), 60.51 (OCH_2), 72.95 (Cb), 127.16 (Cp), 127.61, 128.28, 129.25, 142.45 (Ph), 165.36 (COO); IR (KBr, cm^{-1}) 2975−2863 (ν CH, w), 1716 (ν C=O, s), 1602 (ν C=C, s), 1446 (δ CH_2, w), 1384−1367 (δ CH_3, m), 1273 (ν CO, s), 1175 (m), 1111.0 (s), 1017 (m), 859 (w), 782 (vw), 772, (w), 756 (w), 725 (w), 702 (vw); MS (FAB) *m*/*z* maximum calcd at 2072, found 2075. Anal. Calcd for $C_{55}H_{61}S_5O_8Hg_5Co$: C, 31.88; H, 2.96. Found: C, 31.77; H, 2.86.

Tetra(4-ethoxycarbonylphenyl)cyclobutadienepentakis(acetylthiomercurio)cyclopentadienylcobalt (8). **8** was synthesized from **2** (0.2 g, 0.086 mmol) in THF (5 mL) and thiolacetic acid (0.045 g. 0.59 mmol). Hexanes (60 mL) precipitated **8** (0.13 g, 71%), which was recrystallized from THF/EtOH (dark-red crystals): mp 200−205 °C (dec); ^{1}H NMR δ 7.86 (d, 8 H, J = 8.4 Hz, Ph), 7.79 (d, 8 H, J = 8.4 Hz, Ph), 4.31 (q, 8 H, J = 7.2 Hz, CH_2), 2.26 (s, 15 H, $COCH_3$), 1.32 (t, 12 H, J = 7.2 Hz, CH_3); ^{13}C {^{1}H} NMR δ 14.29 (CH_3), 35.24 (CH_3), 60.50 (CH_2), 74.05 (Cb), 124.40 (Cp), 127.65, 128.74, 129.43, 142.32 (Ph), 165.58 (SCO), 201.05 (COO); IR (KBr, cm^{-1}) 2980 (ν CH, w), 1716 (ν C=O, s), 1637 (s), 1603 (ν Ph, s), 1273 (ν CO, s), 1176 (m), 1111 (s), 1017 (m), 952 (m), 861 (m), 772 (vw), 757 (vw), 726 (vw), 703 (vw), 636 (ν S−CO, m); MS (FAB+) *m*/*z* maximum calcd at 2142, found 2144. Anal. Calcd for $C_{55}H_{51}S_5O_{13}Hg_5Co$: C, 30.84; H, 2.40. Found: C, 31.12; H, 2.40.

Tetra(4-ethoxycarbonylphenyl)cyclobutadienepentakis(2-methylthioethanethiomercurio)cyclopentadienylcobalt (9). **9** was synthesized from **2** (0.2 g, 0.086 mmol) in THF (5 mL) and 2-methylthioethanethiol (0.056 g, 0.52 mmol) in THF (1 mL). Hexanes (50 mL) precipitated **9** (0.13 g, 66%), which was recrystallized from DMSO/EtOH at −20 °C (dark-red crystals): mp 130−135 °C (dec); ^{1}H NMR δ 7.81 (d, 8 H, J = 8.4 Hz, Ph), 7.75 (d, 8 H, J = 8.4 Hz, Ph), 4.30 (q, 8 H, J = 6.9 Hz, OCH_2), 1.96 (s, 15 H, SCH_3), 1.31 (t, 12 H, J = 6.9 Hz, SCH_3); ^{13}C {^{1}H} NMR δ 14.22 (CH_3), 14.48 (CH_3), 26.70 (CH_2), 39.15 (CH_2), 60.53 (OCH_2), 73.10 (Cb), 127.08 (Cp), 127.72, 128.32, 129.33, 142.30 (Ph), 165.34 (COO); IR (KBr, cm^{-1}) 3050 (ν =CH, vw), 2977−2911 (ν −CH, w), 1713 (ν C=O, s), 1602 (ν Ph, s), 1418−1405 (δ CH_2, vw), 1384−1365 (δ CH_3, m), 1272 (ν CO, s), 1175 (m), 1111 (s), 1017 (m), 859 (m), 782 (vw), 772 (vw), 756 (w), 725 (w), 703 (w); MS (FAB+) *m*/*z* maximum calcd at 2302, found 2302. Anal. Calcd for $C_{60}H_{71}S_{10}O_8Hg_5Co$: C, 31.31; H, 3.11. Found: C, 31.41; H, 3.14.

Tetra(4-ethoxycarbonylphenyl)cyclobutadienepentakis(2-acetylthioethanethiomercurio)cyclopentadienylcobalt (10). **10** is synthesized from **2** (0.2 g, 0.086 mmol) in THF (5 mL) and 2-acetylthioethanethiol (0.08 g, 0.59 mmol) in THF (1 mL). Hexanes (60 mL) precipitated **10** (0.11 g, 53%), which was recrystallized from acetone (red crystals): mp 97 °C (dec); ^{1}H NMR δ 7.81 (d, 8 H, J = 8.4 Hz, Ph), 7.74 (d, 8 H, J = 8.4 Hz, Ph), 4.30 (q, 8 H, J = 7.0 Hz, OCH_2), 2.83 (m, 20 H, C_2H_4), 2.30 (s, 15 H, $COCH_3$), 1.31 (t, 12 H, J = 7.0 Hz, CH_3); ^{13}C {^{1}H} NMR δ 14.20 (CH_3), 26.99, 30.63, 34.35, 60.52 (OCH_2), 73.04 (Cb), 126.35 (Cp), 127.71, 128.28, 129.32, 142.38 (Ph), 165.32 (COO), 194.89 (SCO); IR (KBr, cm^{-1}) 2978 (ν CH, vw), 1713 (ν C=O, s), 1693 (ν C=O, s), 1602 (ν Ph, s), 1273 (ν CO, s), 1175 (w), 1112 (s), 1018 (w), 861 (vw), 782, (vw), 772 (vw), 756 (w), 725 (w), 703 (w) 626 (ν S−CO, m); MS (FAB) *m*/*z* maximum calcd at 2443, found 2442. Anal. Calcd for $C_{65}H_{71}S_{10}O_{13}Hg_5Co$·$(CH_3)_2CO$: C, 32.51; H, 3.05. Found: C, 32.66; H, 3.10.

Results and Discussion

The CbCoCp core structure of the cobalt complexes **3**−**12** is the same, and one might expect some underlying commonality in their electrochemical oxidation−reduction processes. However, both the ethoxycarbonyl substituents introduced onto the Cb phenyl groups in **7**−**10** and **12** and the various thiomercurio substituents introduced in **3**−**10** will not only interact with the

TABLE 1: Potentials of Voltammetric Peaks in THF vs Normal Ag/AgC1 Electrode[a]

compd	A	B	C	D	E
11		−2.24			
12		−1.696			−2.16, −2.48
3	−0.80[b]	−2.42[c]		−0.52	
4	−0.69	−(1.9−2.30)[c]		−0.40	
5	−1.14[b]	−2.05	−2.60	−0.80	
6	−0.88[b]	−2.27	−2.50	−0.40[b]	
7	−1.02	−1.72	d	−0.77	−2.10, −2.42
8	−0.75	−1.88[c]		−0.42	−2.33, −2.40
9	−1.10	−1.89	d	−0.67	−2.20, −2.54
10	−1.08[b]	−1.80	d	−0.50	−2.06, 2.66

[a] Ferrocene redox potential was +0.562 V vs this reference electrode. [b] The highest of two or three closely spaced maxima. [c] Peaks B and C are believed to overlap. [d] Peaks C and E are believed to overlap.

organocobalt core and modify its electrochemical behavior but will also be electroactive on their own. A complicated set of properties must be expected.

To acquire sufficient understanding of the oxidation−reduction properties to permit a future investigation of the adsorption of these compounds on mercury, we have examined the compounds by DC and AC polarography, cyclic voltammetry (CV), UV−vis spectroelectrochemistry, and preparative electrolysis. Experiments were performed in two solvents. Solubility in tetrahydrofuran (THF) is adequate for routine electrochemistry in millimolar concentrations. The low dielectric permittivity of THF may suppress adsorption to some extent. In acetonitrile, only 0.1 mM solutions could be prepared. This solvent is likely to promote adsorption and might permit a specification of the potential regions in which adsorbed layers are formed. Presently, we deal only with the elucidation of the fundamentals of the faradaic processes involved.

To facilitate the comparison of related faradaic processes across the series, we denote the electron-transfer reactions by the letters A, B, C, D and E. The last of these reactions comprises two subsequent steps, E_1 and E_2. Roughly speaking, we shall find that these processes correspond to an adsorption-confined reduction (A), "metal-centered" reduction (B), reductive cleavage of tentacles (C), anodic reaction of released tentacles (D), and ester group reduction (E), respectively, but in many instances, these waves and processes cannot be separated neatly and the labels are only approximate. Therefore, the summary of electrochemical potentials of the processes A−E in the 10 compounds given in Table 1 is only an approximate guide.

Parent Complexes 11 and 12. The electrochemical characterization of these two simplest structures is fairly complete. The behavior of **11** is the simplest of all. Both in THF and acetonitrile, DC polarography shows a reversible one-electron reduction at −2.240 V (Figure 1). At 1 mM in THF and 2 s drop time, the limiting current of the well-developed wave is 3.65 μA. Comparison with the wave of ferrocene confirms the consumption of one electron and gives an estimate of the diffusion coefficient, $D = 2.14 \times 10^{-5}$ cm^2•s^{-1}. The wave shape is characterized by a 60 mV/decade slope of the log plot. The corresponding voltammetric curve shows chemical and electrochemical reversibility. The reduction process is accompanied by a substantial change of the UV−vis spectrum observed on a transparent Pt electrode; the 272 nm absorption band of **11** disappears in the fully reduced form, and two new bands at 328 and 412 nm gradually intensify (Figure 2).

Phase-sensitive AC polarography (160 Hz) yields a single reversible faradaic maximum at the half-wave potential, with real and imaginary admittance components of equal height. In

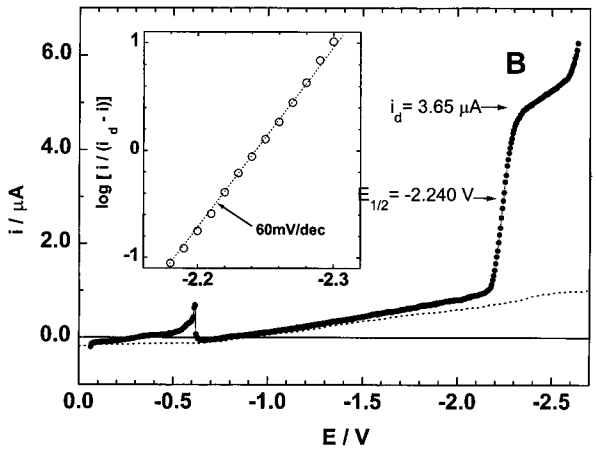

Figure 1. DC polarogram of 1 mM **11** and 0.1 M $TBAPF_6$ in THF (full points) at 2 s drop time: dashed line, blank solution; inset, log plot analysis.

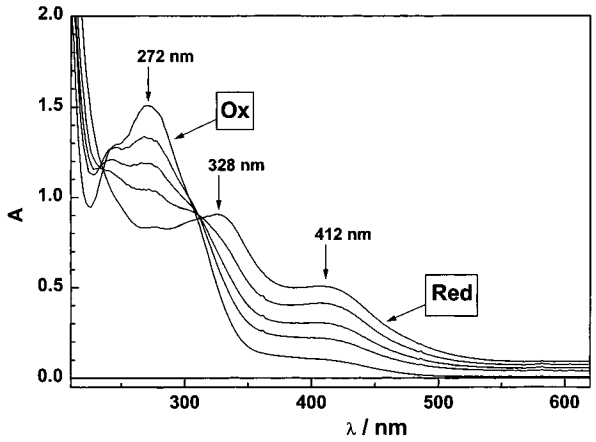

Figure 2. UV−vis spectra of 3 mM **11** in 0.1 M $TBAPF_6$ in THF (thin-layer optically transparent cell, Pt mesh electrode) recorded during a potential scan from −2.0 to −2.5 V: Ox, reactant; Red, fully reduced form.

THF, the presence of **11** changes the double layer capacity C_d only negligibly around 0 V ($C_d = Y''/\omega A$), where Y'' is the imaginary component of the admittance vector Y, ω is the angular frequency of the sine wave perturbation, and A is the electrode area). A small hump at −0.65 V suggests a desorption process that is evidenced also by a discontinuity in Figure 1. In acetonitrile, a substantial lowering of C_d is observed at potentials more positive than −0.5 V. The observed surface activity at positive potentials is attributed to the presence of π-electron-rich ligands on the metal that can interact with a positively charged electrode surface.

We conclude that the observed process involves the uptake of one electron and involves a formation of the radical anion of **11**. This is formally a 19-electron cobalt complex and in principle, might have an 18-electron "slipped-ring" structure[14] in which the Cp ring is only a 4-electron donor (diene-like, with the fifth carbon acting as a free radical center) and the Cb ring acts as a dianion and a 6-electron donor. Since none of our observations demand that such a complication occurs, we assume for the time being that the redox change does not change the molecular geometry substantially.

Formally, the reduction corresponds to going from cobalt(I) to cobalt(0). The degree to which the additional electron actually ends up on the metal center is unclear. In the absence of high-level calculations, we have attempted to obtain a rough idea by performing extended Hückel calculations[15] for several

TABLE 2: Extended Hückel LUMO Energies (eV) and Distributions

compd	*E* (LUMO)		% on Co[a]	% on Cb[b]	% on Cp[c]
11	−9.41		23	62	16
12	−9.79		12	78	10
3	−9.77		3	13	84
7	−9.93		12	59	29
4	(−9.75)[d]	−10.07	0	0	99[e]
8	(−9.94)[d]	−10.08	0	0	99[e]

[a] Contribution of an electron in the LUMO to the total charge on the cobalt atom, in the radical anion (averaged over the two nearly degenerate LUMOs, except in **4** and **8**). [b] Contribution of an electron in the LUMO to the total charge on the cyclobutadiene ring and its substituents, in the radical anion (averaged similarly). [c] Contribution of an electron in the LUMO to the total charge on the cyclopentadienyl ring and its substituents, in the radical anion (averaged similarly). [d] Energy of the orbital that corresponds to the LUMO in **3**, **7**, **11**, and **12**, with d_{xz} and d_{yz} contributions on the Co atom. [e] All concentrated on a single HgSCOMe substituent; there are altogether five approximately degenerate LUMOs spread over the five HgSCOMe substituents.

members of the series at geometries derived from published[2] X-ray structures of CbCoCp complexes and an unpublished[5] X-ray structure of **8**, assuming no Cp ring slipping[14] in the reduced form. The resulting energies of the approximately degenerate lowest unoccupied molecular orbital (LUMO) and their distribution in the molecule are listed in Table 2.

According to the structure of the LUMO in these simple calculations, averaged over the members of the nearly degenerate pair, in **11** the additional electron spends about a quarter of its time on the cobalt atom, most of its time on the tetraphenylated Cb ring, and only a little on the Cp ring. It is therefore likely to be a considerable oversimplification to refer to the reduction as "metal-centered", but in the absence of a better name, we shall adhere to this traditional label. The metal orbitals that participate in the nearly degenerate LUMO are of the d_{xz} and d_{yz} types, where *z* is the ring-center−metal−ring-center direction. These orbitals also participate heavily in the highest occupied molecular orbital (HOMO), and the LUMO corresponds to a metal−ring antibonding orbital.

The tetraester **12** differs from **11** by the presence of an ethoxycarbonyl group in the para position of each phenyl substituent on the Cb ring. The electron-withdrawing COOEt substituents, which themselves are susceptible to reduction, have the expected marked influence on the reduction potential of the metal complex, and **12** yields a well-developed DC polarographic wave at −1.696 V, shifted by 0.540 V to more positive potentials relative to **11**. The limiting current is 2.27 μA, slightly lower than that of **11**, and the estimated diffusion coefficient is $D = 8.3 \times 10^{-6}$ cm^2•s^{-1}. The log plot slope is 60 mV/decade and confirms the reversible nature of the reduction. The LUMO energy of **12** obtained from the extended Hückel calculation is 0.38 eV lower than that of **11**, in surprisingly good semiquantitative agreement with the observed 0.54 eV. According to Table 2, in the radical anion of **12**, the fractional density of the additional electron on the cobalt atom has been reduced somewhat, that on the Cp ring virtually vanished, and the electron now resides almost entirely on the heavily substituted upper deck of the sandwich. This would suggest that substituent shifts on the Cp ring will be less pronounced in **12** than in **11**.

The reversible reduction of **12** at −1.696 V is followed by much larger irreversible polarographic and voltammetric currents at more negative potentials (Figure 3). Irreversible peaks E_1 and E_2 at about −2.15 and −2.45 V, respectively, are assigned

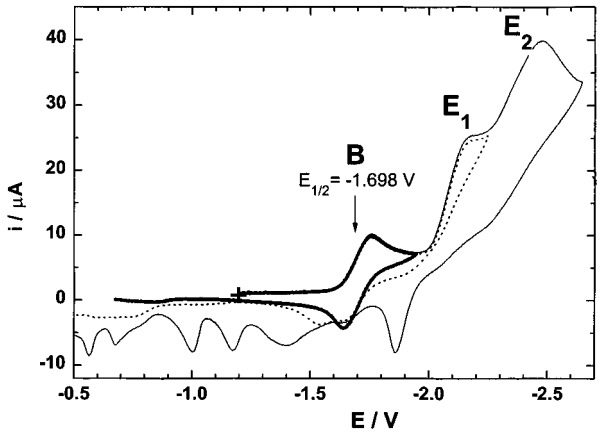

Figure 3. Cyclic voltammograms of 1 mM **12** in 0.1 M $TBAPF_6$ in THF at three different switching potentials; scan rate = 0.5 V/s.

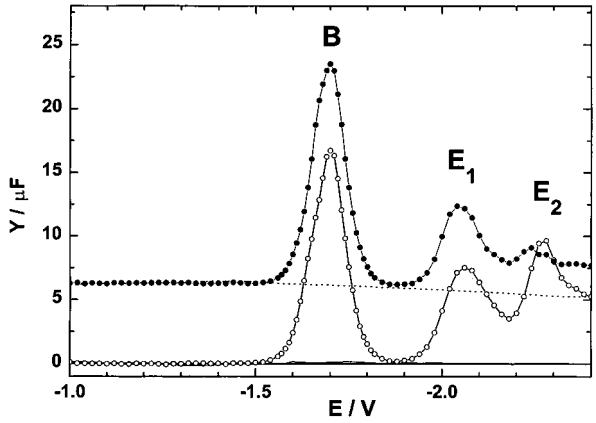

Figure 4. Phase-sensitive AC polarogram of 1 mM **12** in 0.1 M $TBAPF_6$ in THF at 2 s drop time; 160 Hz, amplitude = 5 mV (p−p). Real (empty points, full blank curve) and imaginary (full points, dotted blank curve) components of the admittance are shown.

to the reduction of the ester groups, based on the known reduction of $PhCOOCH_3$ at −2.11 V.[16] When the switching potential is in the range of ester reduction, the back-scan voltammetric curve becomes rather complicated and the reversible peak corresponding to the metal-centered oxidation is almost hidden in overlapping peaks.

The adsorption of **12** from THF solutions is not pronounced. Nevertheless, small humps, similar to those mentioned for **11**, appear at −0.9 V on the DC, AC, and CV curves. This may indicate that the presence of the four ester groups extends the adsorption toward more negative potentials by 0.25 V. The comparison of Figure 3 with the phase-sensitive AC polarogram (Figure 4) demonstrates how, at a suitably chosen frequency, the AC technique differentiates irreversible from reversible faradaic processes. The two admittance peaks at −2.05 and −2.4 V (E_1 and E_2, respectively) are much smaller than the reversible admittance peak B at −1.70 V, although their voltammetric peak currents show just the opposite relation. This feature will help us to locate a reversible reduction overlapped by adjacent irreversible processes for other compounds examined below.

Tentacled Complexes 3−10. The redox behavior of all complexes that carry tentacles on the Cp ligand is much more complicated and not nearly as well understood. All the compounds exhibit certain common features, which have been tentatively assigned to waves A−E in Figure 5 (Table 1). Cathodic faradaic currents observed by DC polarography or cyclic voltammetry occur at about −1 V (wave A), in the

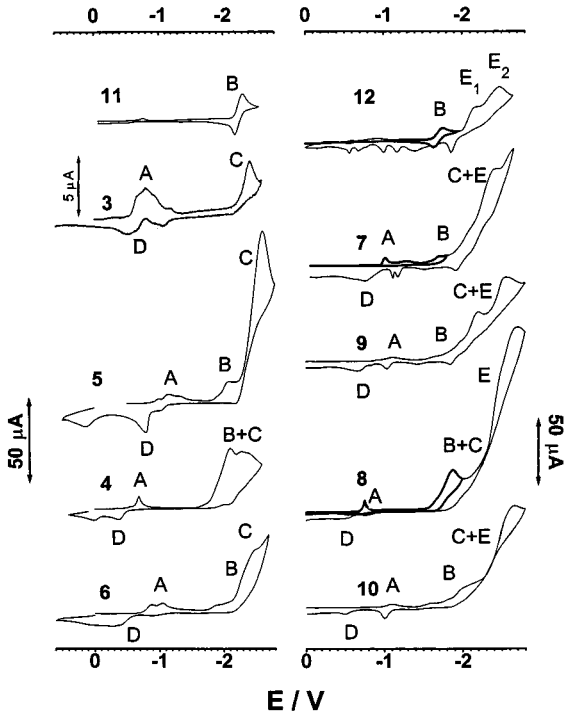

Figure 5. Cyclic voltammograms of **3**−**12** in 0.1 M $TBAPF_6$ in THF at 0.5 V/s scan rate. Concentration: **4**−**7**, **11**, **12**, 1 mM; **8**, **10**, 0.53 mM; **9**, 0.43 mM; **3**, saturated solution, ∼0.04 mM. The 50 μA bar applies to all compounds except for **3**, where the 5 μA bar applies.

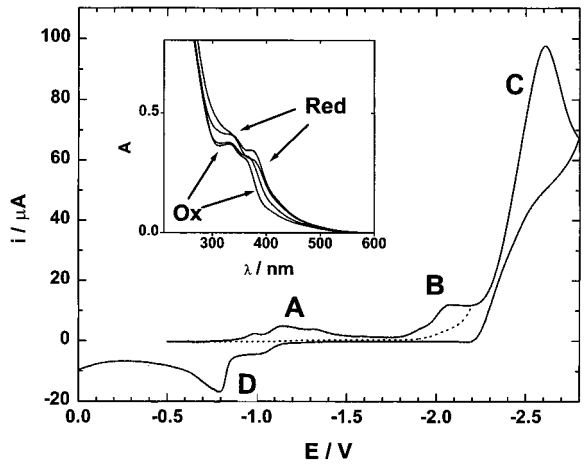

Figure 6. Cyclic voltammetry of 1 mM **5** in 0.1 M $TBAPF_6$ in THF at 0.5 V/s scan rate. Inset shows irreversible changes in the UV−vis spectrum recorded in a spectroelectrochemical cell during the voltage scan of peaks B and C.

potential range of −1.7 to −2.0 V (wave B), and at potentials more negative than −2.2 V (a large wave C or E). A distinct anodic peak (D) common to all tentacled complexes is located in the range −0.4 to −0.8 V.

The behavior is illustrated in results for a typical example, **5** (Figure 6). Irreversible reduction is accompanied by minor changes in the UV−vis spectrum (inset in Figure 6) that are irreversible as well. Complexes with ethoxycarbonyl substituents on the phenyl groups (**7**−**10**, **12**) have an additional complex pattern of anodic peaks, usually dominated by a symmetric peak near −1 V. Since this peak is present in **12** (Figure 3), it is not specifically associated with the presence of tentacles on the Cp ring. Most of these anodic peaks are undoubtedly due to the reduction products of the ester groups. These are of limited interest in this study and we do not attempt to analyze them.

Wave A. This wave corresponds to reduction in the adsorbed state ("adsorption current"). This follows from its nonlinear dependence on the bulk concentration, linear dependence on the scan rate, narrow and symmetrical shape at fast scans, and, for concentrations in the micromolar range, from the dependence of its peak height on the resting time at the initial potential. The resulting reduction product remains strongly adsorbed at potentials between waves A and B, as can be inferred from the low value of the double layer capacity C_d (see below).

Given the only weakly negative potential at which wave A appears, it appears likely that the chemical nature of the reduction is the same as that in wave B of **11** and **12**, i.e., a metal-centered reduction that produces the radical anion of the reactant. This attribution of wave A is supported by the results of preparative electrolysis of **5** at a potential of −1.300 V. After the passage of five electrons per molecule contained in the solution, wave A disappeared and drawn-out anodic waves at −0.4 and −0.1 V were observed. However, 90% of the starting material was subsequently recovered with tentacles intact, and only traces of unidentified products were isolated.

The variation in the position of peak A throughout the series **3**−**10** is undoubtedly related to some degree to the electronic effects of the substituents, but differences in their adsorption properties are likely to play a decisive role. Peak A usually has fine structure in THF and exhibits shoulders or additional CV maxima mainly at the slower scan rates and especially in compounds that contain two sulfur atoms in each of their tentacles. This is most likely related to a time evolution of the adsorbed structure and will be more thoroughly discussed in a future article.[5]

Wave B. Solely on the basis of the general similarity of the position of wave B to those found in **11** and **12**, including a substantial shift to less negative potentials in complexes **7**−**10** that carry ethoxycarbonyl groups at the phenyls, it is likely that the reduction process in the other compounds is the same as that in **11** and **12**. The shift due to the ester groups is smaller than that in the parent compounds with unsubstituted phenyl groups, as expected from the above argument based on extended Hückel calculations. Quantitative comparisons are impossible, both because wave B is doubled in some instances and because it is irreversible and its position is not simply tied to equilibrium properties alone.

In marked contrast to the behavior of **11** and **12**, the reduction process at wave B of **3**−**10** has irreversible character. The waveform is drawn out, the anodic counterpart expected upon scan reversal is completely missing, and CV measurements in THF performed at fast scan rates and/or with different scan switching potentials failed to detect any corresponding anodic reoxidation peak. Spectroelectrochemistry yielded no indication that a stable radical anion is formed, and the UV−vis spectrum resembles that of the reactant at all times (Figure 6). If the reduction process is indeed the same as that in **11** and **12**, metal-centered reduction, we must conclude that the radical anions of the tentacled compounds **3**−**10** are unstable. A likely decomposition path is a loss of one of the tentacles as a thiolate anion in a homogeneous process that could be as simple as a unimolecular dissociation but could also be quite complex. Either way, this would ultimately regenerate the chromophore of the original reactant and account for the spectral results.

In agreement with the assignment of the polarographic wave B to the same metal-centered reduction in all compounds, its height corresponds to a one-electron reduction in **5** and **6**. In **4** and **8**, a much larger current starts already at somewhat less negative potentials, and DC polarographic limiting currents are

approximately 5 times higher. It seems clear that wave C is greatly shifted to less negative potentials and covers up wave B in both of these two cases. The rather facile heterogeneous reduction of the −HgSCOMe moiety is in accord with expectations based on literature data for structurally related compounds.[17−19] Waves B and C also overlap in **3** but at much more negative potentials. In the remaining compounds, **7**, **9**, and **10**, wave B is not covered up by C, but its polarographic limiting current could not be measured reliably.

The effect of the substitution with five −HgSX groups on the ease of the reduction of **11** and **12** shows no clear-cut pattern, and shifts by up to 0.2 V in either direction are observed. This apparent absence of systematic behavior may be due to poor guesses concerning the assignment of wave B in some cases and the irreversible nature of the processes involved in others. In general, it seems that the effect of the tentacles on the reduction of **11** is small and that they make the reduction of **12** a little harder.

It is not obvious a priori what shifts of the half-wave potential should be expected when the five −HgSX substituents are introduced onto the Cp ring. The electropositive nature of the metal atom and the facility of thiol exchange suggest that resonance structures of the type $-Hg^{+-}SX$ are important and that the Hg atoms carry considerable positive charge and cause inductive electron withdrawal. In MO terms, the vacant σ^*_{HgS} orbital has a large amplitude on the Hg atom and acts as an electron density acceptor. Indeed, the inductive substituent constants for this general type of group with an electronegative group X suggest an electron-withdrawing power comparable to that of the ethoxycarbonyl group.[20] Results obtained with the extended Hückel method suggest that the five −HgSMe substituents do not change the nature of the nearly degenerate LUMO, with its characteristic d_{xz}, d_{yz} metal contribution, and stabilize it by 0.36 eV in **11** and 0.15 eV in **12** (Table 2). The difference between the two corresponds to the above qualitative expectations, but the former magnitude appears excessive. The −HgSCOMe substituent is computed to be just as strongly electron withdrawing. Pentasubstitution in **11** to yield **4** stabilizes the metal-centered (d_{xz}, d_{yz}) orbital pair by 0.35 eV, while pentasubstitution in **12** to yield **8** stabilizes the analogous orbitals by 0.15 eV. The similarity of the two substituent effects is not surprising if the effect is primarily due to the polarity of the HgS bond.

The calculations for **4** and **8** are in agreement with the above conclusion that in these two compounds wave C precedes and covers up wave B. According to Table 2, the lowest unoccupied orbitals of the five −HgSCOMe substituents lie well below the metal-centered (d_{xz}, d_{yz}) orbital pair, and they now constitute the several LUMOs of **4** and **8**, at virtually the same energy in both compounds. This is best seen in the distribution of the additional density upon occupying the LUMO, which is calculated to reside exclusively on a single tentacle in both **4** and **8**. It is calculated to lie below the metal-centered orbital by a full 0.32 eV in **4** and by 0.14 eV in **8**, where the metal-centered orbital is stabilized by the four ester groups. This then not only produces a nominal stabilization of the LUMO by 0.66 V upon going from **11** to **4** and by 0.29 V upon going from **12** to **8** but also changes its nature altogether.

Wave C. This also represents an irreversible heterogeneous process. In **5**, the polarographic limiting current corresponds to the overall uptake of 10 ± 1 electrons, suggesting that the process is a complete cleavage of all five tentacles.

$$CbCoC_5(Hg-SX)_5 + 10\ e^- + 5\ H^+ \rightarrow CbCoC_5H_5 + 5\ Hg + 5\ XS^-$$

This is analogous to the previously investigated[17] reduction of $(C_6H_5S)_2Hg$. After a charge corresponding to 10 electrons per solute molecule is passed, preparative electrolysis of **5** at −2.300 V caused the disappearance of the polarographic wave C. Separation of a product from the supporting electrolyte yielded a sample that was identical with **11** by comparison of NMR spectra.

The position of wave C is most clearly defined in **3**−**6**, since the presence of ethoxycarbonyl groups in **7**−**10** causes the appearance of the more complicated overlapping wave or waves E. This also prevents the determination of the number of electrons involved in wave C. Where the position of wave C can be determined, it seems quite constant as would be expected, with the exception of **4** and **8**, already discussed above.

Wave D. This anodic wave is common to all tentacle-carrying complexes but is observed only when the voltammetric switching potential is chosen in the region of wave C, and we assign it to the oxidation of the thiol groups of the free tentacles generated in wave C. This interpretation is supported by the occurrence of peak D also in complexes **3**−**6**, which carry no ester groups; hence, it certainly is not due to their reduction products. The oxidation peak D, though not as sharp, is observed on a gold microelectrode as well.

Waves E. The reduction of the ester groups encountered in **7**−**10** resembles their reduction in **12** and requires no further comment, as it lies outside our present range of interest.

Waves B and C: A Closer Look. The striking irreversibility of the CV wave B in **3**−**10** on stationary electrodes contrasts with the perfectly reversible one-electron metal-centered reduction of **11** and **12** and calls for an explanation. The results of phase-sensitive AC polarography and impedance spectroscopy certainly support the view that the electron transfer at wave B is inherently fast.

In acetonitrile, **5** is about 10 times less soluble than in THF. Acetonitrile enhances adsorption effects, but the behavior in THF is similar. In a CV taken in acetonitrile (Figure 7, top), peak A is higher and sharper, peaks B and D are shifted toward less negative potentials, and peak B is much smaller than C. Wave B is much clearer in AC polarography (Figure 7, bottom). The imaginary and the real AC admittance peaks B at −1.78 V are of equal height and are higher than the AC peaks C at −2.25 V. The imaginary component of peak C is smaller than its real counterpart. According to the theory of the faradaic admittance, equal admittance peaks are expected for a reversible case, whereas for a slow redox process, the imaginary part is smaller than the real part; hence, the irreversibility of wave B observed by CV is due to an EC mechanism and not to a slow electron transfer. Figure 7 also shows that the adsorption of **5** is not a simple process, and four potential regions, marked I−IV, are identified.[5]

The admittance data observed in single-frequency AC experiments were further confirmed by inspection of frequency spectra of electrode impedance (Z) or admittance ($Y = 1/Z$). Peak B is characterized by a frequency spectrum typical of fast electron transfer coupled with the adsorption of reactants.[21] The coupling of redox and adsorption processes is most conveniently displayed as the complex capacitance plot of Y''/ω vs Y'/ω, where Y'' and Y' are the imaginary and the real component of the electrode admittance, respectively (Figure 8). The coupling of the reduction of the metal center with adsorption of the complex yields a capacitance plot composed of part of a quarter circle

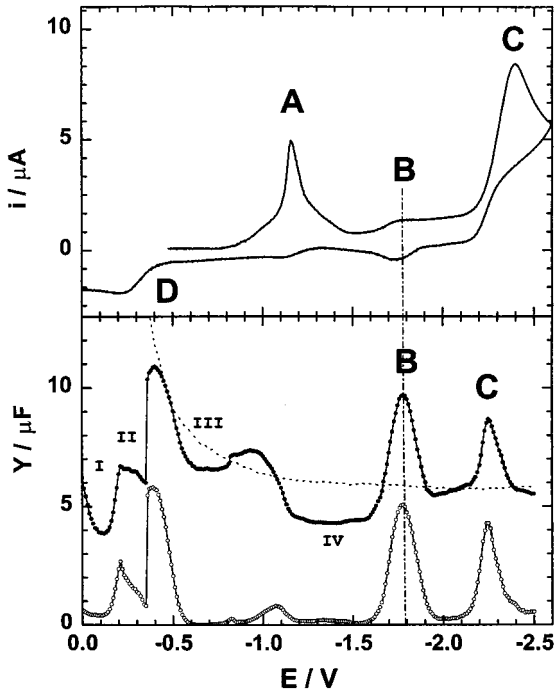

Figure 7. Cyclic voltammogram (top, scan rate 0.5 V/s) and phase-sensitive AC polarogram [bottom, 160 Hz; amplitude = 5 mV (p−p)] of 0.1 mM **5** in 0.1 M $TBAPF_6$ in acetonitrile.

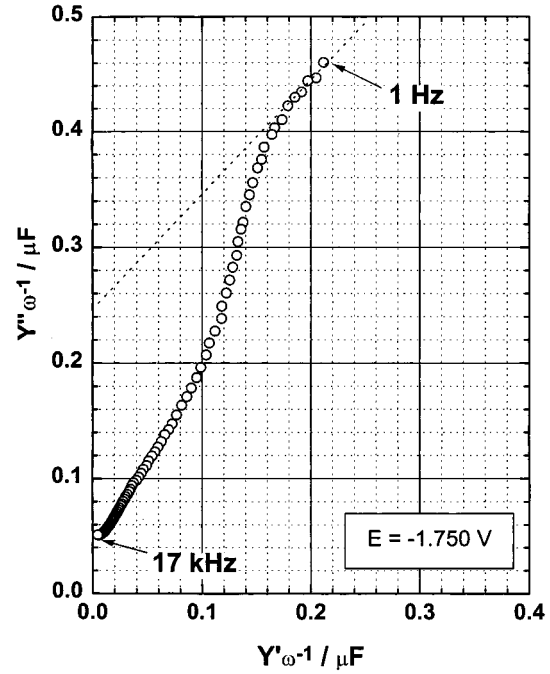

Figure 8. Complex capacitance plot for the solution of Figure 7 at the DC potential of peak B, −1.750 V (corrected for solution resistance, 308.9 Ω, obtained from the high-frequency limit of the complex impedance plot).

and the low-frequency straight line with slope = 1. A simple redox exchange should yield a straight line, either horizontal or tilted at 45°. Pure adsorption/desorption phenomena in the absence of electron transfer would yield only a quarter circle or a semicircle.

The sensitivity with which adsorption effects coupled to the electron-transfer reaction are detected depends on the value of the heterogeneous rate constant k^0. Our previous simulations[22] have shown that frequency dependence such as that in Figure 8 is obtained only for relatively fast redox reactions. The

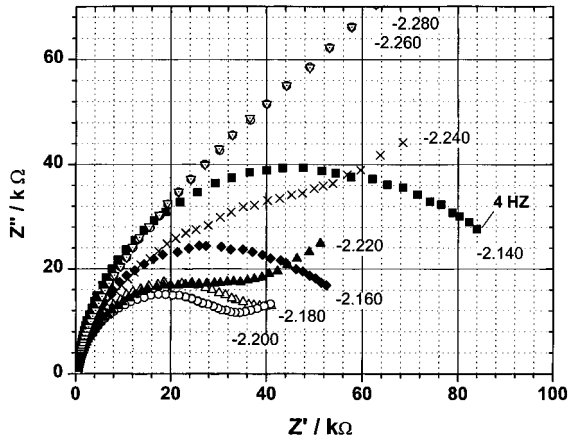

Figure 9. Complex impedance plot for the solution of Figure 7 at DC potentials in the vicinity of peak C: (■) −2.140 V, (◆) −2.160 V, (△) −2.180 V, (○) −2.200 V, (▲) −2.220 V, (×) −2.240 V, (●) −2.260 V, and (▽) −2.280 V.

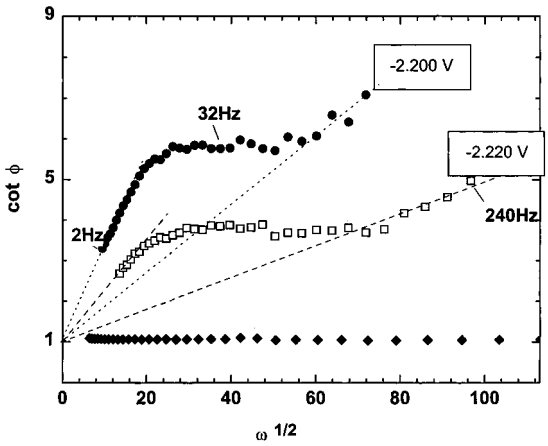

Figure 10. Faradaic phase angle as a function of frequency for the solution of Figure 7 at the two DC potentials shown, close to the half-wave potential (−2.20 V). Corrected for solution resistance (308.9 Ω) and double layer capacitance (4.66 $\mu F \cdot cm^{-2}$). For procedure validation, cf. the reversible behavior of 5 mM ferrocene (◆) in the same medium at its half-wave potential.

frequency dependence of the faradaic peak C from Figure 7 is shown in Figure 9 as the complex impedance plot (Z'' vs Z', where Z'' and Z' are the imaginary and real components of the electrode impedance, respectively). The semicircle shape is different than that observed for peak B and indicates a slow kinetic process limited by diffusion at the lowest frequencies and at the most negative potentials.

The standard treatment[23] of data for peaks B and C involves the evaluation of the imaginary and real component of the faradaic impedance (Z_f'' and Z_f', respectively) by performing a correction for solution resistance (in our cell, typically about 40 Ω in acetonitrile and 330 Ω in THF) and subtraction of the interfacial capacitance ωC_d (where C_d is estimated from the high-frequency limit of the complex capacitance plot). The resulting frequency dependence of the faradaic phase angle ϕ (defined as $\cot \phi = Z_f''/Z_f'$ and shown in Figure 10) permits the estimation of the heterogeneous rate constant from the slope of the high-frequency linear asymptote and yields the value $k^0 = 1.5 \times 10^{-4}$ cm·s^{-1}. The cot plot also indicates the presence of a coupled homogeneous reaction as a low-frequency linear asymptote. This is believed to be the cleavage of tentacles, as confirmed above by preparative electrolysis, and all of the data for wave C thus are in agreement with the proposed interpreta-

tion. Similar large differences in the observed AC reversibility of peaks B and C are observed for other compounds as well.

Conclusions

The parent tetraphenyl-substituted CbCoCp complex **11** undergoes a reversible one-electron reduction at −2.24 V vs Ag/AgCl to yield a radical anion with a characteristic UV−vis spectrum. According to extended Hückel calculations, the additional electron resides in a nearly degenerate metal−ring antibonding orbital, primarily located on the Cb-containing deck ("metal-centered reduction"). Introduction of four ester groups into the para positions of the phenyl substituents on this deck to yield **12** facilitates the reduction by 0.54 V, and the calculations suggest that now the additional electron favors the Cb deck even much more strongly. In addition, at more negative potentials, new reduction waves appear, undoubtedly related to the reduction of the ester groups but not investigated further.

The electrochemical behavior of the derivatives **3**−**10**, which carry five −HgSX tentacles on the Cp ring, is far more complicated. It is characterized by the appearance of an adsorption pre-wave at much less negative potentials, in which the metal-centered reduction takes place and which will be the subject of a separate study. The diffusion-controlled metal-centered reduction still takes place at similar potentials as before, but is now irreversible, and no radical anion spectra have been observed. Presumably, the radical anions of the tentacled species are unstable with respect to the loss of a tentacle in a homogeneous solution process. When the tentacle is −HgSCOMe, its heterogeneous reductive cleavage is so facile that it takes place before the metal-centered reduction can, but the cleavage of tentacles of other structures is observed only at more negative potentials. The cleaved tentacle fragments yield an anodic peak common to all tentacled complexes. Reduction of ester groups is observed at very negative potentials, as in **12**.

Acknowledgment. This work was supported by the Department of Energy (FG03-94ER12141), the National Science Foundation (CTS-9727165), the NATO Scientific and Environmental Division (SRG 951530), and the Grant Agency of the Czech Republic (203/97/1048). T.B. is grateful for a NATO fellowship.

References and Notes

(1) Michl, J. In *Applications of Organometallic Chemistry in the Preparation and Processing of Advanced Materials*; Harrod, J. F.; Laine, R. M., Eds.; Kluwer: Dordrecht, The Netherlands, 1995; p 243. Harrison, R. M.; Magnera, T. F.; Vacek, J.; Michl, J. In *Modular Chemistry*; Michl, J., Ed.; Kluwer: Dordrecht, The Netherlands, 1997; p 1.

(2) Harrison, R. M.; Brotin, T.; Noll, B. C.; Michl, J. *Organometallics* **1997**, *16*, 3401.

(3) Schöberl, U.; Magnera, T. F.; Harrison, R.; Fleischer, F.; Pflug, J. L.; Schwab, P. F. H.; Meng, X.; Lipiak, D.; Noll, B. C.; Allured, V. S.; Rudalevige, T.; Lee, S.; Michl, J. *J. Am. Chem. Soc.* **1997**, *119*, 3907.

(4) Pospíšil, L.; Heyrovský, M.; Pecka, J.; Michl, J. *Langmuir* **1997**, *13*, 6294.

(5) Pospíšil, L.; Fiedler, J.; Brotin, T.; Noll, B. C.; Michl, J. Unpublished results.

(6) Rosenblum, M.; North, B.; Wells, D.; Giering, W. P. *J. Am. Chem. Soc.* **1972**, *94*, 1239.

(7) Gleiter, R.; Röckel. H.; Pflästerer, G.; Treptow, B.; Kratz, D. *Tetrahedron Lett.* **1993**, *50*, 8075.

(8) Schimanke, H.; Gleiter, R. *Organometallics* **1998**, *17*, 275.

(9) Herberich, G. E.; Klein, W.; Kölle, U.; Spiliotis, D. *Chem. Ber.* **1992**, *125*, 1589.

(10) Meade, E. M.; Woodward, F. N. *J. Chem. Soc.* **1948**, 1895.

(11) Rausch, M. D.; Genetti, R. A. *J. Org. Chem.* **1970**, *35*, 3888.

(12) Petukhova, N. P.; Prilezhaeva, E. N. *Zh. Org. Khim.* **1966**, *11*, 1947.

(13) Okuyama, T. *Tetrahedron Lett.* **1982**, *23*, 2665. Okuyama, T. *J. Am. Chem. Soc.* **1984**, *106*, 7134.

(14) Wakatsuki, Y.; Aoki, K.; Yamazaki, H. *J. Chem. Soc., Dalton Trans.* **1982**, *1*, 89. Richards, T. C.; Geiger, W. E. *J. Am. Chem. Soc.* **1994**, *116*, 2028.

(15) Parameters for cobalt, see: Saillard, J.-Y.; Hoffmann, R. *J. Am. Chem. Soc.* **1984**, *106*, 2006. For mercury, see: Underwood, D. J.; Hofmann, R.; Tatsumi, K.; Nakamura, A.; Yamamoto, Y. *J. Am. Chem. Soc.* **1985**, *107*, 5968.

(16) Baizer, M. M., Lund, H., Eds. *Organic Electrochemistry: An Introduction and a Guide*, 3rd ed.; M. Dekker: New York, 1991; p 419.

(17) Person, B.; Nygård, B. *J. Electroanal. Chem.* **1974**, *56*, 373.

(18) Bond, A. M.; Cassey, A. T.; Thackeray, J. R. *J. Electroanal. Chem.* **1973**, *48*, 71.

(19) Toropova, V. F.; Budnikov, R. G. K.; Ulakhovich, N. A. *Talanta* **1975**, *25*, 263.

(20) Exner, O. In *Correlation Analysis in Chemistry*; Chapman, N. B., Shorter, J., Eds.; Plenum Press: New York, 1978; p 439.

(21) Timmer, B.; Sluyters-Rehbach, M.; Sluyters, J. H. *J. Electroanal. Chem.* **1967**, *15*, 343. De Levie, R.; Pospíšil, L. *J. Electroanal. Chem.* **1969,** *22*, 277.

(22) Pospíšil, L. *J. Electroanal. Chem.* **1976**, *74*, 369.

(23) Bard, A. J.; Faulkner, L. R. *Electrochemical Methods, Fundamentals and Applications*; Wiley: New York, 1980; p 338.